CHINESE OPTICS LETTERS

Vol. 19, No. 5 | May 2021

Machine-vision-based acquisition, pointing, and tracking system for underwater wireless optical communications

Jiaming Lin (林佳明)[1], Zihao Du (杜子豪)[1], Chuying Yu (余楚盈)[1], Wenmin Ge (葛文敏)[1], Weichao Lü (吕伟超)[1], Huan Deng (邓 欢)[1], Chao Zhang (张 超)[1], Xiao Chen (陈 潇)[1], Zejun Zhang (张泽君)[1,2,3], and Jing Xu (徐 敬)[1,2,3*]

[1] Optical Communications Laboratory, Ocean College, Zhejiang University, Zhoushan 316021, China

[2] Key Laboratory of Ocean Observation-Imaging Testbed of Zhejiang Province, Ocean College, Zhejiang University, Zhoushan 316021, China

[3] The Engineering Research Center of Oceanic Sensing Technology and Equipment, Ministry of Education, Zhejiang University, Zhoushan 316021, China

*Corresponding author: jxu-optics@zju.edu.cn

Received August 6, 2020 | Accepted November 27, 2020 | Posted Online February 24, 2021

Due to the proliferation of underwater vehicles and sensors, underwater wireless optical communication (UWOC) is a key enabler for ocean exploration with a strong reliance on short-range bandwidth-intensive communications. A stable optical link is of primary importance for UWOC. A compact, low-power, and low-cost acquisition, pointing, and tracking (APT) system is proposed and experimentally demonstrated to realign the optical link within 0.04 s, even when the UWOC transmitter and receiver are in relative motion. The system successfully achieves rapid auto-alignment through a 4 m tap water channel with a relatively large number of bubbles. Furthermore, the required minimum illumination value is measured to be as low as 7.1 lx, implying that the proposed APT scheme is robust to dim underwater environments. Meanwhile, mobility experiments are performed to verify the performance of the APT system. The proposed system can rapidly and automatically align moving targets in complex and unstable underwater environments, which can potentially boost the practical applications of UWOC.

Keywords: acquisition; pointing and tracking; underwater wireless optical communication.

DOI: 10.3788/COL202119.050604

1. Introduction

Due to the world's increasing population and expanding industries in recent decades, the ocean has become a promising venue to seek additional resources. The number of deployed autonomous underwater vehicles (AUVs) has increased dramatically, which relies on high-bandwidth and low-latency underwater communication technologies[1]. Although tremendous progress has been made in the field of underwater acoustic communication in the past few decades, its bandwidth (< 1 MHz) and propagation speed ($\sim$1500 m/s) are extremely limited[1]. This has led to the proliferation of underwater wireless optical communication (UWOC), as it can provide higher data rates than traditional acoustic communication systems with a significantly lower power consumption and simpler computational complexity for short-range wireless links[1,2]. Recently, important findings on UWOC have been discovered[3–9]. In 2017, Li *et al.* demonstrated a 16 Gbps UWOC at an underwater transmission distance of 10 m using four-level pulse amplitude modulation (PAM4)[4]. In 2019, Wang *et al.* used the non-return to zero (NRZ) on–off keying (OOK) modulation method and achieved 100 m/500 Mbps using a 520 nm laser diode (LD)[7]. These high-speed and long-distance UWOC systems require precise alignment. However, AUV movement disturbs the optical communication link connection in real scenarios. Therefore, there are still some acquisition, pointing, and tracking (APT) issues that need to be solved for UWOC systems before they can be applied to real underwater environments.

Some APT systems have been proposed and experimentally demonstrated in the field of visible light communications (VLCs)[10–14]. These can be divided into two main categories: received-signal-strength-indicator (RSSI)-based and visual-based APT methods. The RSSI-based APT system uses an optical sensor to detect the signal strength and localize it using standard trilateration by leveraging three anchors (light sources)[11]. This type of system, such as the system in Ref. [12], may have a limited underwater performance due to additional interference with light sources, such as that from glowing marine life or directly from the AUVs. The visual-based APT system uses a camera/image sensor to align the transmitter and receiver by image processing[13]. Such a system provides mobility and can achieve quick indoor alignment[14]. In 2016, a team proposed to track the motion and activities of humans and objects by projecting visible light onto people and objects to create

shadows[11]. Since shadows do not necessarily exist in the underwater environment, this method may not be applicable underwater. In 2019, scientists designed a simple and effective tracking scheme for VLC systems, which used a beacon light and a camera as core components of the APT system to successfully establish an optical path for communication[13]. In the same year, an innovative APT system using ceiling mirrors, the beacon light, and cameras was proposed and demonstrated for data centers[14]. However, the high hardware cost and power consumption brought by the extra beacon light may inhibit their use in underwater energy-sensitive conditions. The underwater environment is more complex and unpredictable than its indoor counterpart, especially when considering some underwater-specific interference sources that further affect the UWOC performance, such as bubbles generated by the AUV motion, ambient light, water turbidity, and the mirror surface produced by the air–water interface[15–17].

In this work, an APT system is developed to solve the issues associated with UWOC mobility. The proposed APT system can be conveniently integrated into existing UWOC systems, and it is much simpler than the traditional APT system for VLC. The UWOC transmitter is fixed on the camera in the APT system, and a specific mark is attached to the surface of the UWOC receiver. The operation of the APT system is based on identifying and tracking the special mark. More importantly, to the best of our knowledge, the effects of the underwater environment on the APT system were studied in this work for the first time, including ambient light, attitude transformation, water turbidity, and bubbles. Moreover, the proposed APT system can be widely used in UWOC systems due to its compact, low-power, low-cost, and open-source nature. In water with a distance of 6 m, the APT system has been demonstrated to realign the system within 0.04 s, even when the UWOC transmitter and receiver are in relative motion. As a result, the APT system has been proven to have the ability to quickly and automatically align under dim and bubbly underwater environments. This work not only provides an innovative approach to UWOC mobility issues but also offers a broad perspective for UWOC deployment in real environments.

2. Experimental Setup and Details

The proposed APT system includes a 300,000 pixel OpenMV camera with servos and a specific mark called the AprilTag. The OpenMV camera is an open-source machine vision module that integrates the STM32H743VI ARM Cortex M7 chip with a 400 MHz clock frequency, 1 MB random access memory (RAM), and 2 MB flash. AprilTag is a visual fiducial mark that is useful for a wide variety of tasks, including augmented reality, robot positioning, and camera calibration[18–21]. The machine vision code runs on an STM32H743VI chip and computes the precise three-dimensional (3D) position, orientation, and identity of the mark. The real-time and low-power operation can be readily achieved on inexpensive embedded devices. The main mark detection process includes the detection of quad

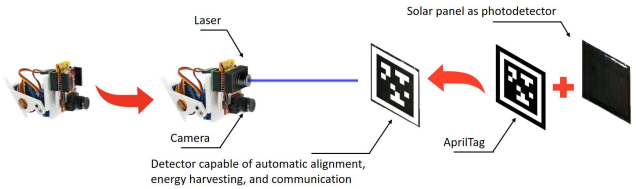

Fig. 1. Structure diagram showing an example of how to combine the existing UWOC system with the proposed APT system.

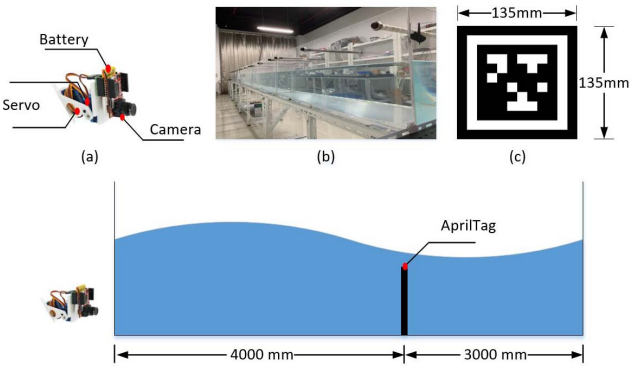

Fig. 2. Experimental setup of the proposed APT system for UWOC. Insets: (a) the camera with servos, (b) the water tank, and (c) the AprilTag36H11-2.

from captured images and the following process, where each candidate is further decoded to determine if they are valid AprilTag detections[20]. Figure 1 shows an example of how to combine the existing UWOC system with the proposed APT system. As the third part focuses on the performance of the APT system, UWOC setup appears in the fourth part only.

Figure 2 depicts the experimental setup of the proposed APT system, which is implemented in a water tank with dimensions of 300 mm × 400 mm × 7000 mm. An OpenMV camera with servos is situated on the left to find and track the target. A printed AprilTag is placed in a water tank 4 m away from the camera to simulate the receiving terminal of a UWOC system.

3. Experimental Results

We first measured the pointing time at different distances when the illumination in front of the camera was fixed at 410.5 lx. The time required for each calibration was measured, and the results were output through the microcontroller to reduce the errors caused by manual operations. Figure 3(a) indicates that as long as the target remains in the field of view, the pointing time is nearly the same, with a value of approximately 41.8 ms. It is noted that the pointing time was measured, while the function to calculate the target rotation angle was turned on, and the video and data were reported to the computer. If these functions are not necessary in actual use, the response time will be further reduced. Moreover, a greater APT distance requires higher resolution photos, which requires cameras with a larger number of pixels. When operating beyond the maximum distance

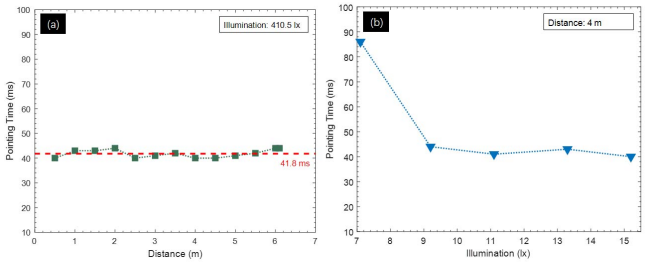

Fig. 3. Influence of different factors on the pointing time showing (a) the pointing time of the proposed APT system measured in the underwater channel at different distances and (b) the pointing time of the proposed APT system measured in the underwater channel at different illuminations.

permitted by the camera, the captured image is blurred, and the APT fails. Since a higher resolution requires additional processing time, there is a trade-off between the APT distance and the operation time.

We explored the relationship between the illumination level and the pointing time. The primary factors affecting indoor underwater illumination are the overhead fluorescent lamps and sunlight entering through the window, as shown in Fig. 2(b). Therefore, to prevent the interference from those factors, we turned off all indoor fluorescent lamps and drew the curtains. At this time, the underwater illumination was 0.4 lx, and then we used an adjustable lamp as the only light source for quantitative analysis. The measured results are shown in Fig. 3(b). The system cannot run properly until the illumination reaches 7.1 lx, and the pointing time drops to 40 ms when the illumination exceeds 9.2 lx. This conclusion indicates that the system can tolerate a wide illumination range and can operate in dim underwater environments.

In order to evaluate the effects of attitude transformation in actual environments on the proposed APT system, we used the roll/yaw/pitch angle to characterize the impacts of different attitude transformations (see Fig. 4 for a schematic diagram).

To measure the impact of each angle individually, we conducted three experiments to measure the system's pointing time in the underwater channel at different roll angles, yaw angles, and pitch angles, respectively. In the first experiment, we measured the relationship between the roll angle and the pointing time, while fixing the yaw angle and pitch angle to zero. The measured results are shown in Fig. 5. The roll angle increases from 0 to 360 deg, and the pointing time remains around

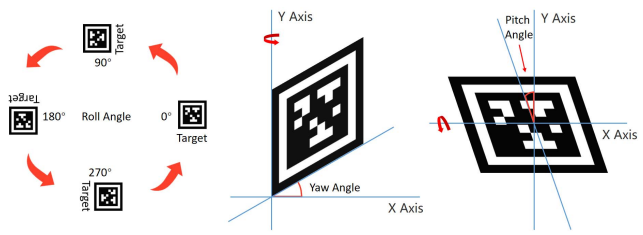

Fig. 4. Schematic diagram of roll angle, yaw angle, and pitch angle.

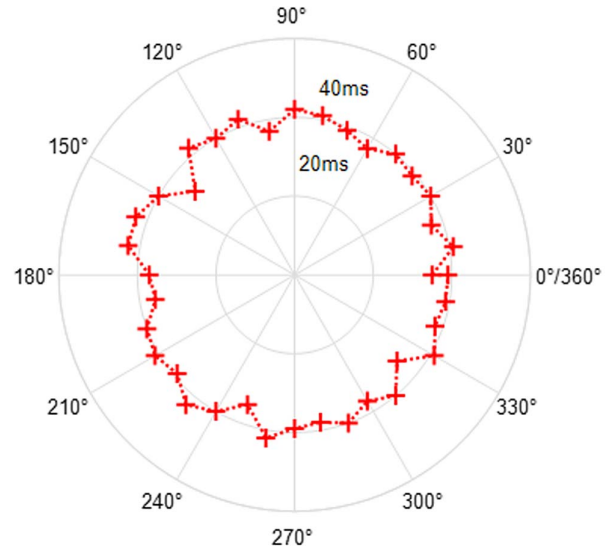

Fig. 5. Pointing time of the proposed APT system measured in the underwater channel at different roll angles.

39.2 ms, demonstrating the robustness of the proposed scheme to the variation of roll angle.

In the next experiment, we fixed the roll angle and pitch angle to be equal to zero and changed the yaw angle. When the yaw angle is zero, the target is facing directly towards the camera; as the yaw angle approaches 90 deg, the target rotates out of view, and the APT system loses the ability to point. As can be seen from Fig. 6(a), the maximum allowable yaw angle is about 60 deg, and the pointing time is almost fixed at a constant value of about 40.4 ms within the allowable yaw angle range.

The complementary experiment held the roll angle and yaw angle equal to zero and changed the pitch angle. The measured results are shown in Fig. 6(b). The range of the pitch angle is similar to the range of the yaw angle, with a value of about 60 deg. The pointing time maintains about 39.9 ms, and the pitch angle continues to grow from 0 to 60 deg. These three experiments on roll/yaw/pitch angle prove that the proposed APT system can cope with attitude changes, further expanding the application range of the system.

To estimate the effects of bubbles in actual underwater environments for the proposed APT system, we used the scintillation coefficient to characterize the effects of different bubble sizes and

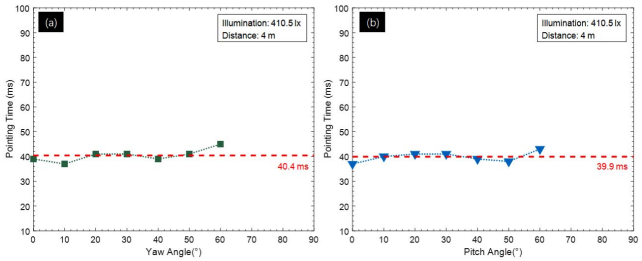

Fig. 6. Pointing time of the proposed APT system measured in the underwater channel (a) for different yaw angles and (b) for different pitch angles.

densities. The optical power meter and energy meter (Thorlabs, PM200) were set to record 1000 points for each scenario. By monitoring the variations in the received intensity from one sample to another, we calculated the scintillation index[22], $\sigma_I^2(\lambda)$, as

$$\sigma_I^2(\lambda) = \frac{\langle I^2(\lambda)\rangle - \langle I(\lambda)\rangle^2}{\langle I(\lambda)\rangle^2}, \quad (1)$$

where $I(\lambda)$ is the received intensity for the wavelength λ, and the angle brackets denote the time-average operator.

We used the pump to adjust the intake air and furthermore altered the scintillation index, whose relation with pointing time is shown in Fig. 7. These results suggest that the APT system has a tolerance for bubbles; this is primarily due to the characteristics of the recognition algorithm, which has certain anti-pollution abilities[18].

We further considered the ability of the APT system to track the target at different speeds. Unfortunately, the electronically controlled slide, without any waterproofness, cannot be deployed underwater. Therefore, we performed the experiments indoors with a set distance between the rail and the APT system of 5 m and an illumination level of 373.2 lx. The light in the room came primarily from the lamps overhead and the sunlight through the windows. The tracking time for different moving speeds of the target is measured and shown in Fig. 8(a). The maximum speed at which the system could still track was not measured due to the rail speed limitation. However, the measurements were sufficient to show that the system can continually and rapidly track targets with a moving speed up to 3.9 cm/s. These results indicate that the mobility limitations in typical UWOC systems can be compensated for using the proposed APT system.

We finally verified the acquisition capability of the system. In this scheme, we used the rectangular spiral scanning method, which is shown in Fig. 9(a). The rectangular spiral scans sequentially from the center to the outside. There are two main advantages of this scanning method. The first advantage is that the scanning range in this way can cover all parts of the target area. This is mainly used for the primary acquisition, without any known information. The second advantage is that it can scan from high-probability areas to low probability areas to minimize tracking time. For example, after establishing the pointing, the target quickly moves to the right, resulting in loss. At this time, the system searched around the last disappeared place according to the movement trend of the target. Here, the time required for the first acquisition was measured. A schematic diagram of the experimental setup scene is shown in Fig. 9(b). In previous experiments, the target was placed in the field of view of the camera. However, we next placed the target outside the field of view and allowed the system to automatically control the servos to acquire the target. The critical parameter is the deviation angle α between the target and the optical axis of the camera. The target moved horizontally and continually, which caused different deviation angles, and the required time for each deviation angle was recorded, as shown in Fig. 8(b). We conclude from Fig. 8(b) that the deviation angle significantly affects the acquisition time.

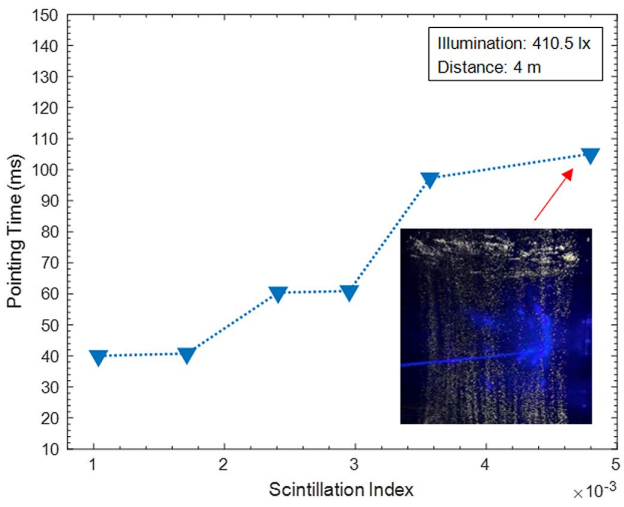

Fig. 7. Pointing time of the proposed APT system measured in the underwater channel with different scintillations.

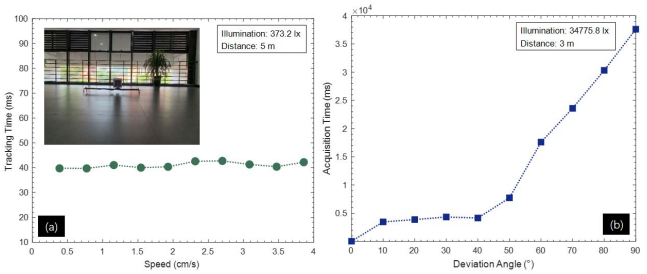

Fig. 8. Influence of different factors on the tracking/acquisition time showing (a) the tracking time of the proposed APT system measured in a 5 m air channel at different speeds and (b) the acquisition time of the proposed APT system measured in a 3 m air channel at different angles.

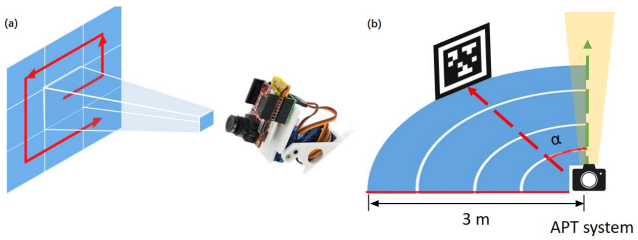

Fig. 9. (a) A schematic diagram of the APT system acquiring a target and (b) the experimental setup for the acquisition time measurement at different deviation angles (α). The yellow area is the camera's field of view, and the green line is the optical axis of the APT system.

4. Proof-of-Concept Experiments

As mentioned above, the proposed APT system can be simply integrated into the UWOC system. In this part, we have conducted a proof-of-concept experiment to demonstrate both the APT and communication capabilities of the integrated

system, based on the setup in Fig. 10. Firstly, the NRZ-OOK signals were loaded into an arbitrary waveform generator (AWG) (SIGLENT, SDG5122). The AWG sampling rate was set at 4 MSamples/s, and the AWG output amplitude was clipped within $5V_{pp}$. The baseband modulation OOK signal was superimposed on direct current via a drive circuit. After these processes, the OOK signal was transmitted by using a 445 nm LD mounted on the APT system. Then, we printed an AprilTag with a size of 51 mm × 51 mm, subtracted its black part, and pasted the rest of the white part on the solar panel with a size of 131 mm × 61 mm. A water tank with dimensions of 195 mm × 225 mm × 285 mm was placed between the integrated transmitter and integrated receiver to act as a proof-of-concept underwater channel. After transmitting through a tap water channel, the optical OOK signals were received by the special solar panel. The detected signals were captured by an oscilloscope (GW Instek, GDS-3254) with a sampling rate of 125 MSamples/s. Finally, the captured signals were demodulated by MATLAB.

Initially, the camera of the APT system pointed at the bottom of the water tank. Meanwhile, the special solar panel was fixed in the center of the opposite side of the water tank, out of the camera's field of view. Then, the APT system began to acquire the special solar panel. After 574 ms, the optical link of the UWOC system had been automatically established, with the corresponding eye diagram being measured. After the pointing process had been completed, we randomly selected another time point, say after 614 ms, to measure the eye diagram again. The measured UWOC eye diagrams of these two time points are shown in Fig. 11(a). Both eye diagrams are wide open, verifying that the communication link is stable.

Next, magnesium hydroxide powder was added to the water to change the turbidity. We gradually increased the concentration of magnesium hydroxide powder and recorded the corresponding pointing time, as shown in Fig. 11(b). The pointing time increases as the concentration of magnesium hydroxide powder increases. When the concentration of magnesium hydroxide powder exceeds 226.18 mg/L, the APT system fails. Communication has been maintained during this period, although the light intensity has dropped 100 times.

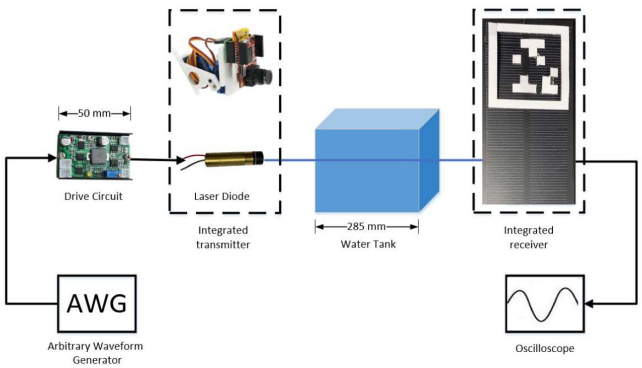

Fig. 10. Experimental setup for proof-of-concept experiments for the proposed APT system integrated into a UWOC system.

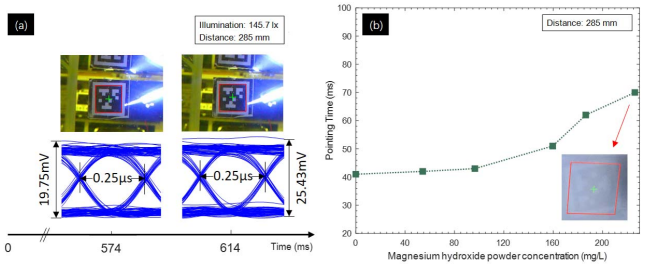

Fig. 11. (a) Eye diagrams of the integrated system using NRZ-OOK modulation after acquiring the target through a 285 mm water channel, and (b) the pointing time of the proposed APT system measured in the underwater channel with different magnesium hydroxide powder concentrations.

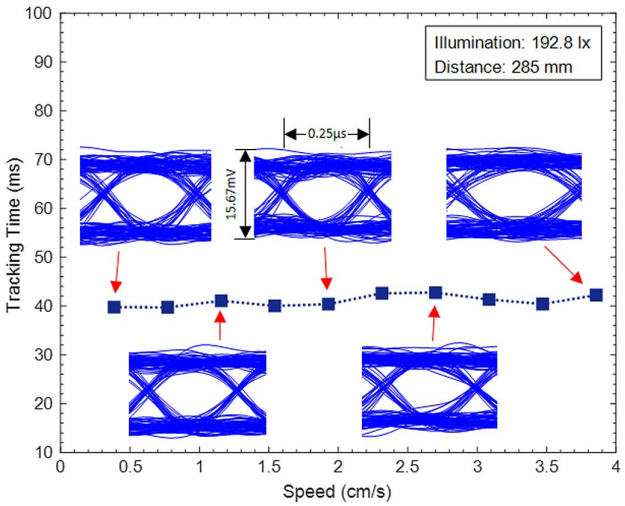

Fig. 12. Eye diagrams of the integrated system using NRZ-OOK modulation during tracking the target through a 285 mm air channel.

Finally, we investigated the communication performance during the tracking process. Since the electronically controlled slide is not waterproof, we removed the water tank while maintaining the distance at 285 mm. The integrated receiver was fixed on the slide and moved at different speeds. The eye diagrams during tracking are shown in Fig. 12, again verifying that the communication link is stable even when the transmitter and receiver are in relative motion. In exploring higher communication rates by using solar panels, other scientists have made significant progress. For example, cheap solar cells were used in UWOC, achieving 84 Mbps using quadrature amplitude modulation (QAM)[23]. In addition, the flexibility of the solar panel permits it to be attached to the surface of AUVs to achieve the high-speed UWOC, APT, and the energy harvesting.

5. Conclusion

We demonstrated an effective APT system for practical UWOC. In this design, representative factors in real underwater environments are considered. The effects of distance, illumination,

attitude transformation, bubbles, speed, and angle on the APT performance were systematically investigated. For the given example in this study, the response times for APT are approximately 40 s, 0.04 s, and 0.04 s, respectively. The proposed system has been verified underwater, including the tolerance for bubbles and the feasibility under an illumination level as low as 7.1 lx. In addition, the proposed system features a compact footprint, low power, low cost, and open source. The system was further integrated with a UWOC system, demonstrating continuous and stable APT capabilities. This research provides an essential step towards the realistic deployment of UWOC systems.

Acknowledgement

This work was supported by the National Natural Science Foundation of China (NSFC) (Nos. 61971378 and 61671409), National Key Research and Development Program of China (Nos. 2016YFC1401202, 2017YFC0306601, and 2017YFC0306100), and Strategic Priority Research Program of the Chinese Academy of Sciences (No. XDA22030208).

References

1. H. Kaushal and G. Kaddoum, "Underwater optical wireless communication," IEEE Access **4**, 1518 (2016).
2. J. Xu, "Underwater wireless optical communication: why, what, and how? [Invited]," Chin. Opt. Lett. **17**, 100007 (2019).
3. Y. Chen, M. Kong, T. Ali, J. Wang, R. Sarwar, J. Han, C. Guo, B. Sun, N. Deng, and J. Xu, "26 m/5.5 Gbps airwater optical wireless communication based on an OFDM-modulated 520-nm laser diode," Opt. Express **25**, 14760 (2017).
4. C. Li, H. Lu, W. Tsai, M. Cheng, C. Ho, Y. Wang, Z. Yang, and D. Chen, "16 Gb/s PAM4 UWOC system based on 488-nm LD with light injection and optoelectronic feedback techniques," Opt. Express **25**, 11598 (2017).
5. X. Liu, S. Yi, X. Zhou, Z. Fang, Z. Qiu, L. Hu, C. Cong, L. Zheng, R. Liu, and P. Tian, "34.5 m underwater optical wireless communication with 2.70 Gbps data rate based on a green laser diode with NRZ-OOK modulation," Opt. Express **25**, 27937 (2017).
6. S. Hu, L. Mi, T. Zhou, and W. Chen, "35.88 attenuation lengths and 3.32 bits/photon underwater optical wireless communication based on photon-counting receiver with 256-PPM," Opt. Express **26**, 21685 (2018).
7. J. Wang, C. Lu, S. Li, and Z. Xu, "100 m/500 Mbps underwater optical wireless communication using an NRZ-OOK modulated 520 nm laser diode," Opt. Express **27**, 12171 (2019).
8. N. Chi and F. Hu, "Nonlinear adaptive filters for high-speed LED based underwater visible light communication [Invited]," Chin. Opt. Lett. **17**, 100011 (2019).
9. C. Li, H. Lu, Y. Huang, Q. Huang, J. Xie, and S. Tsai, "50 Gb/s PAM4 underwater wireless optical communication systems across the water–air–water interface [Invited]," Chin. Opt. Lett. **17**, 100004 (2019).
10. S. Wen, X. Cai, W. Guan, J. Jiang, B. Chen, and M. Huang, "High-precision indoor three-dimensional positioning system based on visible light communication using modified artificial fish swarm algorithm," Opt. Eng. **57**, 106102 (2018).
11. M. Ibrahim, V. Nguyen, S. Rupavatharam, M. Jawahar, and R. Howard, "Visible light based activity sensing using ceiling photosensors," in *Proceedings of VLCS'16 Proceedings of the 3rd Workshop on Visible Light Communication Systems* (ACM, 2016), pp. 43.
12. L. Huang, P. Wang, Z. Liu, X. Nan, L. Jiao, and L. Guo, "Indoor three-dimensional high-precision positioning system with bat algorithm based on visible light communication," Appl. Opt. **58**, 2226 (2019).
13. F. Liu, W. Jiang, X. Jin, and Z. Xu, "A simple and effective tracking scheme for visible light communication systems," Proc. SPIE **11048**, 110481H (2019).
14. F. Liu, M. Chen, W. Jiang, X. Jin, and Z. Xu, "Effective auto-alignment and tracking of transceivers for visible-light communication in data centres," Proc. SPIE **10945**, 109450N (2019).
15. L. Chen, Y. Shao, and R. Deng, "Robust UOWC systems against bubble-induced impairments via transmit/receive diversities [Invited]," Chin. Opt. Lett. **17**, 100006 (2019).
16. P. Tian, H. Chen, P. Wang, X. Liu, X. Chen, G. Zhou, S. Zhang, J. Lu, P. Qiu, Z. Qian, X. Zhou, Z. Fang, L. Zheng, R. Liu, and X. Cui, "Absorption and scattering effects of Maalox, chlorophyll, and sea salt on a micro-LED-based underwater wireless optical communication [Invited]," Chin. Opt. Lett. **17**, 100010 (2019).
17. X. Huang, F. Yang, and J. Song, "Hybrid LD and LED-based underwater optical communication: state-of-the-art, opportunities, challenges, and trends [Invited]," Chin. Opt. Lett. **17**, 100002 (2019).
18. E. Olson, "AprilTag: as robust and flexible visual fiducial system," in *Proceedings of IEEE International Conference on Robotics and Automation* (IEEE, 2011), p. 3400.
19. A. Richardson, J. Strom, and E. Olson, "AprilCal: assisted and repeatable camera calibration," in *Proceedings of IEEE/RSJ International Conference on Intelligent Robots and Systems* (IEEE, 2013), p. 1814.
20. J. Wang and E. Olson, "AprilTag 2: efficient and robust fiducial detection," in *Proceedings of IEEE/RSJ International Conference on Intelligent Robots and Systems* (IEEE, 2016), p. 4193.
21. M. Krogius, A. Haggenmiller, and E. Olson, "Flexible layouts for fiducial tags," in *Proceedings of IEEE/RSJ International Conference on Intelligent Robots and Systems* (IEEE, 2019), p. 1898.
22. O. Alkhazragi, X. Sun, V. Zuba, E. M. Amhoud, H. Oubei, T. K. Ng, B. Jones, M.-S. Alouini, and B. S. Ooi, "Spectrally resolved characterization of thermally induced underwater turbulence using a broadband white-light interrogator," IEEE Photon. J. **11**, 7905609 (2019).
23. X. Chen, W. Lyu, C. Yu, Y. Qiu, Y. Shao, C. Zhang, M. Zhao, J. Xu, and L. Chen, "Diversity-reception UWOC system using solar panel array and maximum ratio combining," Opt. Express **27**, 34284 (2019).